
Effects of Electrode Materials on Charge Conduction Mechanisms of Memory Device Based on Natural Aloe Vera

Zhe Xi Lim, Sasidharan Sreenivasan, Yew Hoong Wong, Feng Zhao and Kuan Yew Cheong

MRS Advances / *FirstView* Article / July 2016, pp 1 - 6
DOI: 10.1557/adv.2016.522, Published online: 21 July 2016

MRS Advances © 2016 Materials Research Society
DOI: 10.1557/adv.2016.522

Effects of Electrode Materials on Charge Conduction Mechanisms of Memory Device Based on Natural Aloe Vera

Zhe Xi Lim[1], Sasidharan Sreenivasan[2], Yew Hoong Wong[3], Feng Zhao[4] and Kuan Yew Cheong[1]

[1]Electronic Materials Research Group, School of Materials & Mineral Resources Engineering, Engineering Campus, Universiti Sains Malaysia, 14300 Nibong Tebal, Penang, Malaysia.
[2]Institute for Research in Molecular Medicine, Universiti Sains Malaysia, 11800 Minden, Penang, Malaysia.
[3]Department of Mechanical Engineering, Faculty of Engineering, Universiti Malaya, 50603 Kuala Lumpur, Malaysia.
[4]Micro/Nanoelectronics and Energy Laboratory, School of Engineering and Computer Science, Washington State University, Vancouver, WA 98686, U.S.A.

ABSTRACT

Resistive switching behaviors in Aloe vera films are being explored for nonvolatile memory applications. A simple structure in which the Aloe vera films sandwiched in between a top and bottom electrode are used. The switching behaviors of the devices in which the Aloe vera film is dried at different temperatures and the roles of top electrode materials (Al and Ag) are investigated. Current density–voltage measurements reveal that filamentary conduction is the dominant conduction process inducing resistive switching characteristics in Aloe vera films. Device with Al-top electrode requires a forming voltage higher than devices with Ag-top electrode, due to the tendency of oxide formation of these materials. The resistive switching behaviors are highly reproducible, as demonstrated by the data retention performance over an interval of 10^4 s and endurance capability of over 100 cycles.

INTRODUCTION

As technology evolves rapidly, the useful lifespan of electronics is getting shorter. An electronic device tends to be replaced by new substitutes with more advanced functions before reaching the end of operational lifespan [1]. This planned obsolescence of electronic devices can lead to severe environmental issues as vast amounts of electronic waste (e-waste) resulted from disposal of electronic devices can overwhelm landfills around the world [2]. The increasing awareness towards sustainable development is opening up opportunities to explore the possibility of using bio-organic materials for electronic applications [3,4].

One of the bio-organic materials that demonstrate potential for electronic applications is Aloe vera (*Aloe barbadensis* Miller). Although traditional applications of Aloe vera for various medicinal, cosmetic, and nutritional purposes are well established [5], its uses in electronic applications remain relatively unexplored. Aloe vera as a bio-organic material offers unique advantages, such as its abundance in nature, biodegradability, and biocompatibility, which are not easily replicated by other materials. Aloe vera can be a promising candidate for electronic applications as electrostimulation of living Aloe vera plants can induce traceable electrical responses [6]. Furthermore, thin films of commercial Aloe vera gel have been used as natural dielectrics [7] in organic field-effect transistors (OFETs) [8] to showcase its potentials for viable electronic applications. Recently, the demonstration of inducing responses that mimic memristor behaviors in living Aloe vera plants has further expanded its potentials for electronic memory applications [9]. The notion has been conceptualized when thin films of commercial [10] and natural [11] Aloe vera gel are explored for nonvolatile memory applications.

The bipolar switching in thin films of natural Aloe vera gel are attributed to charge trapping and detrapping processes as charges are transported across the Aloe vera film via space-charge-limited conduction (SCLC) [11]. In contrary, many reports [12-20] attribute the resistive switching behaviors in thin films of bio-organic materials to the formation and dissolution of a conductive filament bridging the top and bottom electrodes. The memory cells typically consist of an active (e.g. Ag), an ion-conducting layer, and an inert electrode (e.g. ITO). The principle operation of these memory cells is based on the fact that bio-organic materials extracted from living organisms are excellent ion conductors, depending on their preparation conditions and the top electrode plays a major role in the filamentary conduction. In this paper, an experiment is conducted to investigate if resistive switching behaviors due to filamentary conduction can be induced in thin films of natural Aloe vera gel for nonvolatile memory applications. The role of top electrode in relation to the filamentary conduction is also examined by using Al and Ag as the top electrodes of the Aloe vera-based memory device.

EXPERIMENTAL

The Aloe vera gel and samples were prepared according to the procedures described elsewhere [11]. Two sets of samples were prepared, using Al and Ag as the top electrodes of the devices. The top electrodes are of circular shape with a diameter of 0.1 cm and consequently an effective cell area of 7.85×10^{-3} cm^2. Electrical characteristics of the devices were measured at normal ambient conditions using a Semiconductor Parameter Analyzer (Agilent 4156C). The device under measurement was placed on a probe station (Lake Shore TTP4) and bias voltages were applied to the top electrode while the bottom electrode was grounded in all measurements. A compliance current of 1 mA was imposed.

RESULTS AND DISCUSSION

Figure 1a,b show the typical current density–current (*J*–*V*) characteristics of the Aloe vera-based memory devices. The devices are having a simple ITO/Aloe vera/(Al or Ag) bottom-up structure. Both of them exhibit resistive switching behaviors suitable for nonvolatile memory applications. In a typical measurement, the bias voltages were applied on the top electrode, while the bottom electrode was grounded. The bias voltages were swept according to the sequences: (i) 0 → 10 V, (ii) 0 → –1 V, (iii) –1 → 0 V, (iv) 0 → 1 V, and (v) 1 → 0 V. During the first voltage sweep, the devices undergo a forming process where an abrupt increase in current density can be detected at 9.8 V and 4.6 V for devices using Al and Ag as the top electrode respectively (insets of Figure 1a,b). This abrupt increase in current density indicates that the devices have undergone the transition from a high-resistance OFF-state to a low-resistance ON-state. The devices can be switched from the ON-state back to the original OFF-state (reset process) at –0.6 V during the second voltage sweep. Subsequent state transition (set process) can only occur in the fourth voltage sweep, where a smaller bias voltage (0.3 V and 0.6 V for devices using Al and Ag as top electrode respectively) is required to toggle the device as compared to the first voltage sweep. The sequence of voltage sweeps employed here is different from the previous report [11] causing significant differences in the *J*–*V* characteristics. In this paper, a forming process is required to prepare the pristine device for subsequent switching cycles. Moreover, the set and reset voltages

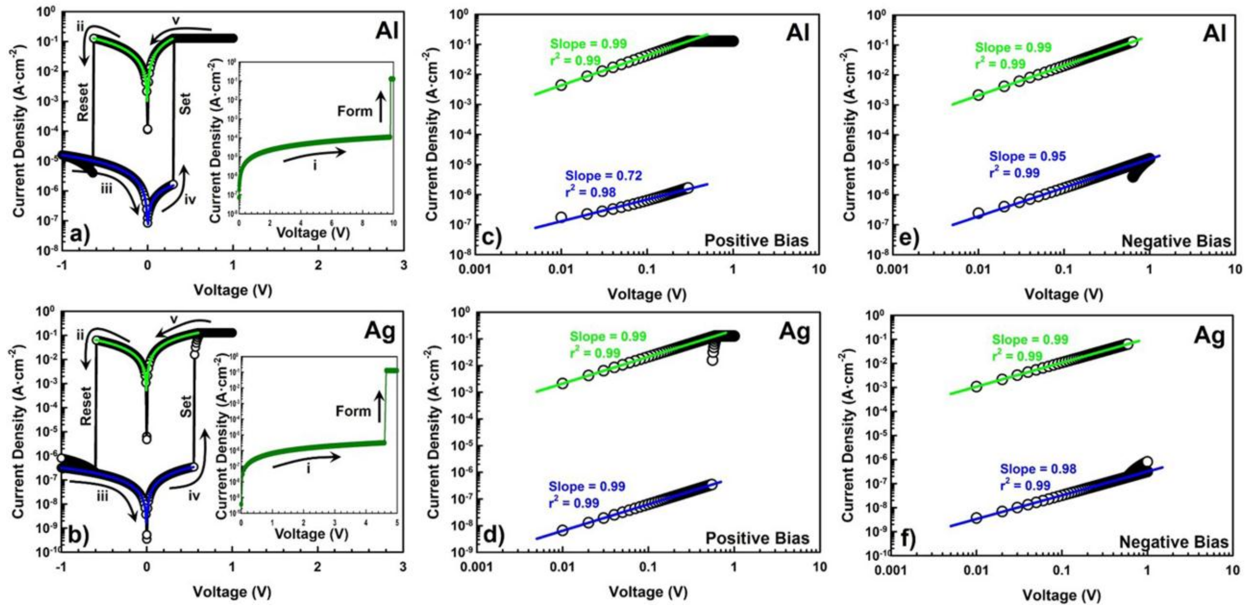

Figure 1. Typical *J–V* characteristic curves of the a) ITO/Aloe vera/Al and b) ITO/Aloe vera/Ag device. Insets show the initial forming process of the corresponding device. Arrows indicate the direction of voltage sweeps and their sequence is numbered using Roman numerals. Log-log plot of the *J–V* characteristics in b,c) positive bias and e,f) negative bias regions of the corresponding device. Solid lines are linear fittings of Ohm's law to the experimental data.

reported here occur at lower magnitude and at opposite polarity of the previous report [11], suggesting that the resistive switching behaviors can be induced by different conduction mechanisms.

To elucidate the governing charge conduction mechanism, the *J–V* characteristics are replotted in logarithmic scale and the experimental data is fitted according to Ohm's law. The linear *J–V* relationships with slopes of close to 1 in the positive (Figure 1c,d) and negative (Figure 1e,f) regions indicate that Ohmic conduction is dominant in both ON- and OFF-state of the devices. These observations imply that the conduction mechanism is associated to the formation and rupture of a conductive filament [12-20] within the Aloe vera films. In contrast, the *J–V* characteristics of the device reported previously [11] depict three distinct regions in both positive and negative bias, which can be fitted with a combination of Ohm's and Child's law (OFF-state), and Child's law (ON-state), respectively, constituting the framework of SCLC theory.

In the previous report [11], the switching behaviors show a strong dependency on the drying temperature of Aloe vera films. The switching behaviors can only be induced in Aloe vera film dried at 50°C but not for other drying temperature. Drying temperature above and below this point can alter the intermolecular interactions of polysaccharides in the Aloe vera films, causing unfavorable conditions for SCLC. Here, the drying temperature of Aloe vera films shows no profound effect on the resistive switching behaviors, as switching can still be induced even when the Aloe vera films are dried at temperatures higher than 50°C. Figure 2a,b show the variations of ON/OFF ratio and read voltage window for Aloe vera films processed at different drying temperatures. The slight variation of both parameters, as the drying temperature increases, is insignificant. To verify the existence of localized filaments within the Aloe vera film, memory cells with varying effective area were fabricated. Figure 2c shows the relationships between

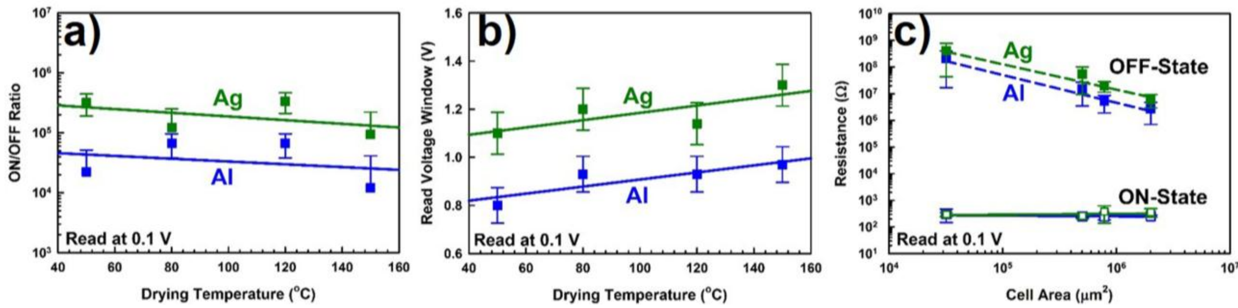

Figure 2. Effects of drying temperature of the Aloe vera films on a) ON/OFF ratio and b) read voltage range of the device. c) Cell area dependency of the ON- and OFF-state resistances.

OFF- and ON-state resistances and the effective cell area. In the OFF-state, the current is presumed to flow homogenously throughout the entire cell area, causing to the increase of resistance (R) with decreasing cell area (A) that follows the relationship of $R \propto 1/A$. In contrary, the ON-state resistance is independent of the cell area since most of the current is flowing in the localized filament connecting the bottom and top electrodes. This result is in agreement with other reports [16,21].

Figure 3 shows the illustrations of filamentary conduction processes that give rise to the resistive switching behaviors. In the pristine device (Figure 3a), device with Al top electrode contains more metal ions than the devices with Ag top electrode. This is because Al has a higher standard electrode potential ($\Delta E° = +1.66$ V) as compared to Ag ($\Delta E° = –0.8$ V) [22]. Thus, Al electrode tends be oxidized into metal ions and diffused into the Aloe vera film. Besides that, a discontinuous layer of oxide is also formed at the Al/Aloe vera interface. While dense and continuous interfacial is critical in inducing switching [23-26], this interfacial AlO_x layer serves no major roles. As a voltage is applied, metal ions in the Aloe vera films drift towards the negatively biased bottom electrode (Figure 3b). The metal ions arriving at the bottom interface is reduced

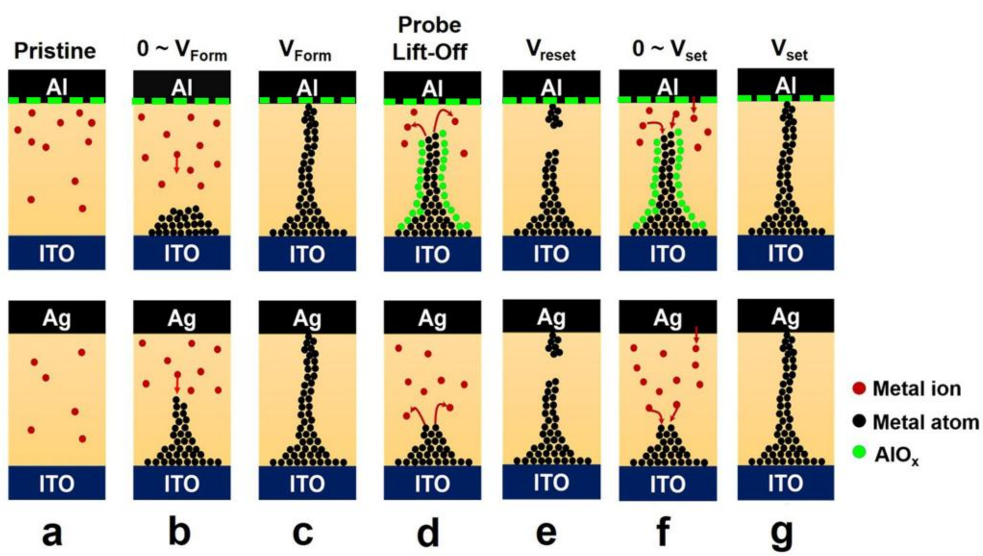

Figure 3. Schematics illustrating the resistive switching behavior a) in a pristine device, b) when a voltage is applied on the top electrode, c) forming process, d) probe lift-off incident, e) reset process, and f,g) set process.

back to neutral atoms. This reduction process is not occurring at the same rate, as Al ions tend to combine with oxidants in the bulk to form AlO_x. The forming process is done when a complete filament is formed within the Aloe vera film (Figure 3c). The measuring probe is lifted (Figure 3d) causing the dissociation of filaments via oxidation into metal ions. Due to its higher oxidation tendency, a thin AlO_x layer surrounding the filament prevents successive oxidation of the Al filament. The filaments can be destroyed by applying a negative voltage (Figure 3e). The filament can be reformed by applying a positively bias voltage (Figure g,h).

Figure 4a shows the data retention characteristics of the device under a continuous 0.1 V voltage stress. The device maintains good data retention characteristics as no significant degradation of current density in both ON- and OFF-state can be observed throughout the stress test interval. To examine the endurance performance, the device is toggled between its two states over 100 cycles (Figure 4b). Although some variations in the OFF-state current density can be observed, the device is able to maintain an ON/OFF ratio of 10^3 over 100 cycles. The cumulative probability of the set and reset voltages is shown in Figure 4c. The set voltages show a larger variation as compared to the reset due to the random and localized nature of filament growth.

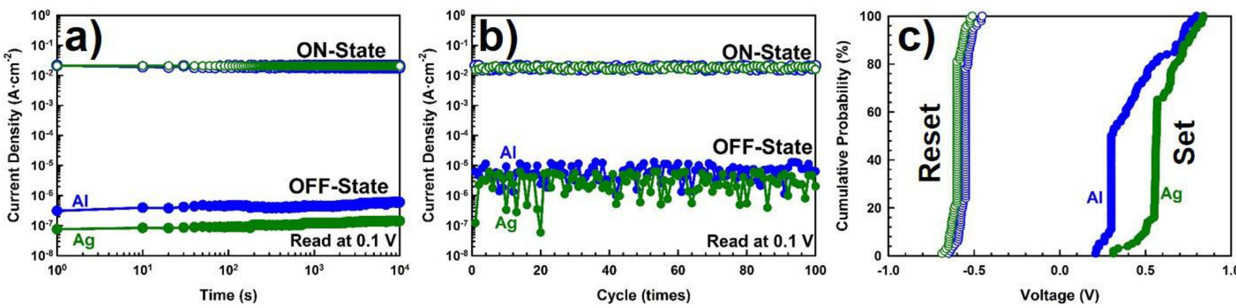

Figure 4. a) Data retention characteristics of the device under a continuous 0.1 V voltage stress and b) endurance performance of the device over 100 ON/OFF cycles. c) Cumulative probability distribution of operating voltages for set and reset processes.

CONCLUSIONS

In summary, resistive switching behaviors in thin films of Aloe vera gel are being explored for nonvolatile memory applications. The switching behaviors are independent of the drying temperature of the Aloe vera films. Linear fittings of the *J–V* characteristic curves lead to the deduction that the governing conduction mechanism is associated with the electrochemical growth and dissolution of filaments within the Aloe vera films. The top electrode plays a critical role in introducing metal ions into the Aloe vera films and subsequently contributes positively to the filamentary conduction. A high forming voltage of 9.8 V is required when Al top electrode is used, as the naturally formed interfacial oxide layer serves as an extra barrier for metal ion generation at the interface. The forming voltage can be lowered to 4.6 V when Ag to electrode is used instead. The resistive switching behaviors are highly reproducible, as demonstrated by the data retention performance over an interval of 10^4 s and endurance capability of over 100 cycles.

ACKNOWLEDGMENTS

This work was supported by Fundamental Research Grant Scheme (no. 6071301), USM Research University–Individual Grant (no. 814216), and USM Postgraduate Research Grant

Scheme (no. 8036018). Z. X. Lim would like to acknowledge the scholarship given by Ministry of Higher Education Malaysia under MyBrain15–MyPhD Program.

REFERENCES

1. S. Bauer and M. Kaltenbrunner, *ACS Nano* **8**, 5380-5382 (2014).
2. M. Irimia-Vladu, *Chem. Soc. Rev.* **43**, 588-610 (2014).
3. S. Mühl and B. Beyer, *Electronics* **3**, 444-461 (2014).
4. N. Savage, *IEEE Spectrum* **52**, 18 (2015).
5. E. R. Rodríguez, J. D. Martín and C. D. Romero, *Crit. Rev. Food Sci. Nutr*. **50**, 305-326 (2010).
6. A. G. Volkov, J. C. Foster, E. Jovanov and V. S. Markin, *Bioelectrochemistry* **81**, 4-9 (2011).
7. L. Q. Khor and K. Y. Cheong, *J. Mater. Sci. Mater. Electron.* **24**, 2646-2652 (2013).
8. L. Q. Khor and K. Y. Cheong, *ECS J. Solid State Sci. Technol.* **2**, P440-P444 (2013).
9. A. G. Volkov, J. Reedus, C. M. Mitchell, C. Tucket, V. Forde-Tuckett, M. I. Volkova, V. S. Markin and L. Chua, *Plant Signaling Behav.* **9**, e29056 (2014).
10. W. F. Lim, H. J. Quah, S. Sreenivasan and K. Y. Cheong, *Mater. Technol.* **30**, A29-A35 (2015).
11. Z. X. Lim and K. Y. Cheong, *Phys. Chem. Chem. Phys.* **17**, 26833-26853 (2015).
12. Y. Ko, Y. Kim, H. Baek and J. Cho, *ACS Nano* **5**, 9918-9926 (2011).
13. H. Baek, C. Lee, K.-I. Lim and J. Cho, *Nanotechnology* **23**, 155604 (2012).
14. M. K. Hota, M. K. Bera, B. Kundu, S. C. Kundu and C. K. Maiti, *Adv. Funct. Mater.* **22**, 4493-4499 (2012).
15. N. Gogurla, S. P. Mondal, A. K. Sinha, A. K. Katiyar, W. Banerjee, S. C. Kundu and S. K. Ray, *Nanotechnology* **24**, 345202 (2013).
16. K. Nagashima, H. Koga, U. Celano, F. Zhuge, M. Kanai, S. Rahong, G. Meng, Y. He, J. De Boeck, M. Jurczak, W. Vandervorst, T. Kitaoka, M. Nogi and T. Yanagida, *Sci. Rep.* **4**, 5532 (2014).
17. Y.-C. Chang and Y.-H. Wang, *ACS Appl. Mater. Interfaces* **6**, 5413-5421 (2014).
18. N. R. Hosseini and J.-S. Lee, *ACS Nano* **9**, 419-426 (2014).
19. Y.-C. Chen, H.-C. Yu, C.-Y. Huang, W.-L. Chung, S.-L. Wu and Y.-K. Su, *Sci. Rep.* **5**, 10022 (2015).
20. N. R. Hosseini and J.-S. Lee, *ACS Appl. Mater. Interfaces* **8**, 7325-7332 (2016).
21. X.-J. Zhu, J. Shang and R.-W. Li, *Front. Mater. Sci.* **6**, 183-206 (2012).
22. D. R. Lide, *CRC Handbook of Chemistry and Physics*, 84th ed. (CRC Press, Bota Raton, FL, 2004) ch. 8, pp. 23-28.
23. T. Oyamada, H. Tanaka, K. Matsushige, H. Sasabe and C. Adachi, *Appl. Phys. Lett.* **83**, 1252 (2003).
24. M. Cölle, M. Büchel and D. M. de Leeuw, *Org. Electron.* **7**, 305-312 (2006).
25. F. Verbakel, S. C. J. Meskers, R. A. J. Janssen, H. L. Gomes, M. Cölle, M. Büchel and D. M. de Leeuw, *Appl. Phys. Lett.* **91**, 192103 (2007).
26. T. Kever, U. Böttger, C. Schindler and R. Waser, *Appl. Phys. Lett.* **91**, 083506 (2007).